GENERATION OF CONSISTENT NUCLEAR PROPERTIES OF DUPIC FUEL BY DRAGON WITH ENDF/B-VI NUCLEAR DATA LIBRARY

Wei Shen and Daniel Rozon
Institut de Genie Nucleaire
Ecole Polytechnique de Montreal
C.P. 6079, Succ. Centre-ville
Montreal (Quebec), Canada H3C, 3A7

ABSTRACT

DRAGON code with 89-groups ENDF/B-VI cross section library was used in this paper to generate consistent nuclear properties of DUPIC fuel. The reference feed material used for the DUPIC fuel cycle is a 17x17 French standard 900 MWe PWR spent fuel assembly with 3.2 w/o initial enrichment and 32500 MWD/T discharge burnup. The PWR fuel assembly was modeled by JPMT/SYBILT transport method in DRAGON to generate nuclide fields of spent PWR fuel. The resultant nuclide fields constitute the initial fuel composition files for reference DUPIC fuel which can be accessed by DRAGON for CANDU 2D cluster geometry depletion calculation and 3D supercell calculation. Because of uneven spatial power distribution in PWR assemblies and full core, unexpected transition cycle, and various fuel management strategy, the spent PWR fuel composition is expected to be different from one assembly to the next. This heterogeneity was characterized also by modeling various spent PWR fuel assembly types in the paper.

I. INTRODUCTION

The concept of the DUPIC (Direct Use of Spent PWR fuel in CANDU reactor) fuel cycle is to reuse the spent PWR fuel in CANDU reactor by an oxidation and reduction of oxide fuel (OREOX) process, which is technically feasible and safeguardable.[1] The study of DUPIC fuel cycle in CANDU reactor requires the pre-calculation of few group homogenized cross sections of DUPIC cluster cell and in-core reactivity devices such as adjuster rods and Zone Control Units(ZCUs). Because the fresh DUPIC fuel is made of spent PWR fuel, not only the typical CANDU cluster cell and supercell but the PWR assembly have to be modeled by a lattice code.

In the previous studies,[2] the nuclear properties of DUPIC fuel were generated by different lattice code with various libraries: the composition of spent PWR fuel was calculated by CASMO-3 based on ENDF/B-IV, the base cross sections of DUPIC cell was obtained by WIMS-AECL based on ENDF/B-V, and the incremental cross sections of in-core reactivity devices was generated by separate 3D transport code SHETAN. In addition, the ORIGEN code had to be used to link the CASMO-3 and WIMS-AECL codes.

The advanced lattice analysis code DRAGON[3] was designed for general geometry and can analyze both CANDU clusters and PWR assemblies. It also has the capability to do three-dimensional supercell transport calculations. It contains three modules for self-shielding calculation and transport calculation: (1) JPMT module: interface current method applied to homogeneous blocks (2) SYBILT module: collision probability method for simple 1D or 2D geometry and the interface current method for 2D Cartesian or hexagonal assemblies (3) EXCELT module: collision probability method for more general 2D geometry and for 3D assemblies. To overcome the drawbacks of using inconsistent computational codes and corresponding libraries of previous studies, the DRAGON code with an 89-groups ENDF/B-VI cross section library was used in this paper to generate consistent nuclear properties of DUPIC fuel in three steps:

Step 1: 2D PWR assembly depletion and cooling calculation to generate the nuclide field of spent PWR fuel.
Step 2: 2D CANDU cluster geometry depletion calculation to generate the burnup-dependent few group base cross sections of DUPIC fuel.
Step 3: 3D CANDU supercell transport calculation to get incremental cross sections of in-core reactivity device in CANDU core.

CANDU 2D cluster cell and 3D supercell analysis made by DRAGON has been introduced before,[4] hence we shall emphasis our effect on 2D PWR assembly modeling, benchmark, nuclide fields generation, and observed fuel composition heterogeneity discussion. In addition, we will compare our results with those generated based on ENDF/B-V library of previous study.[5]

II. CHARACTERISTICS OF REFERENCE PWR FUEL

A 17x17 French standard 900 MWe PWR Fuel was used as reference PWR fuel for the DUPIC fuel cycle study. The geometrical descriptions of two types of assemblies, i.e., fuel assembly without burnable poison (BP) and BP assembly, are showed in Figures 1 and 2. The fuel assembly comprises 264 fuel rods distributed over 289 cell locations in an eight-of-square symmetry. This assembly has three distinct types of cell, 264 fuel rod cells, one instrumentation cell and 24 guide tube cells. The BP assembly consists of 16 BP rods inserted into the 16 guide tube locations. We thus obtain four different types of cells for BP assembly. The general parameters of French standard 900 MWe PWR are summarized in Table 1:

Table 1: Characteristics of 900 MWe PWR Fuel

• Core Performance

Rated power (MWth)	2895
Number of assemblies	157
Active core height	366 cm
Loading strategy	
3 batch, 52-feed assemblies: out-in	
Feed enrichment	3.2 w/o

• Assembly Characteristics

Assembly type	17x17
Assembly pitch	21.504 cm
Uranium weight	461.42 kg
Water gap width	0.042 cm
BP material	Pyrex

• Fuel Pellet Characteristics

Fuel rod diameter	0.819 cm
Theoretical density	10.412 g/cm^3
Thickness of clad diameter	0.057 cm
Clad material	Zircaloy 4
Density of Zr-4	6.55 g/cm^3

• Coolant Temperature (°C)

Hot zero power	291.4
Core average, hot full power	310.7

III. DRAGON PWR ASSEMBLY MODELING

Numerical results show that a pin cell model is not enough to represent the whole 17x17 PWR assembly as it underestimates assembly eigenvalue more than 10%. In order to obtain a reliable nuclide field, we should model the 17x17 assembly in 2D and calculate the flux distribution inside the assembly correctly. We will now describe and justify the main calculation options that were used in DRAGON for PWR assembly modeling. The technique selected is a compromise between precision and calculation speed.

Library: our calculations were performed using the ENDF/B-VI WIMS-AECL format library since it is a more recent library and it contains the most important isotopes for the study of DUPIC fuel cycle in CANDU reactor. The transport correction is applied in a fashion similar to WIMS-AECL.

Geometry: 1/8 symmetric two-dimensional (2D) 17x17 PWR assemblies with and without BP were simulated by applying a reflective boundary. The narrow water gap between each assembly is included, but the spacer and grid is not considered, as their contributions on fuel composition can be neglected. The fuel cells were divided into 3 annular regions: fuel, clad (void is homogenized with clad) and moderator. BP rod cells were divided into 6 annular regions: SS304 (mixed with air gap), BP rod, SS304, moderator, clad and moderator.

Self-Shielding: The self-shielding calculations were performed using the same geometry as that used in the transport calculation. The collision probabilities required for self-shielding calculations were calculated using JPMT module without Livolant-Jeanpirre normalization. This option was selected based on the benchmark calculations discussed in next section.

Transport Calculation: The collision probabilities required for transport calculations were performed using SYBILT module.

Buckling And Leakage: Because of large leakage both in the radial and axial directions we felt that a K-infinity eigenvalue calculation would not be reliable. Accordingly, we performed a flux calculation with critical buckling search using the B1 homogeneous leakage method for PWR depletion calculation. The corrected form of B1 model is treated as a positive correction to total cross section without having to recompute the collision probabilities. The correction is performed by multiplying the collision probabilities by a non-leakage probability at the flux solution level. This is the approach we selected for our calculation by using the option PNL in the flux solution module.

IV. DRAGON BENCHMARK FOR STATIC PWR LATTICE

The DRAGON code has been benchmarked against CANDU design codes, and results compare well with experimental data.[6] In order to evaluate the accuracy of DRAGON with the model described above for a PWR lattice, calculations were performed using the JPMT/SYBILT (JPMT module for self-shielding calculation and SYBILT module for transport calculation) neutron transport method with four different options:

Option 1: Self-shielding without Livolant-Jeanpirre(LJ) normalization, ENDF/B-VI library.
Option 2: Self-shielding with LJ normalization, ENDF/B-VI library.
Option 3: Self-shielding without LJ normalization, ENDF/B-V library.

Option 4: Self-shielding with LJ normalization, ENDF/B-V library.

A. PWR Pin Cell

In recent papers,[7-9] Doppler coefficients of reactivity for an infinite lattice of slightly idealized PWR pin cells were calculated using MCNP-3A and MCNP-4A Monte Carlo code with ENDF/B-V, and ENDF/B-VI libraries. These results were used as a set of numerical benchmarks to evaluate the accuracy of DRAGON code for PWR pin cell. The studied cases are pin cells representative of 17 x 17 PWR lattices at hot zero power (600 K) and hot full power (900 K) with 1400 ppm boron in the moderator. The temperature for cladding and moderator is 600 K in all cases, and there is no thermal expansion of dimensions. Only fuel temperature and number densities are changed for different power levels. Five enrichments, from natural uranium to 3.9 wt%, and two plutonium cases representative of depleted fuel were studied.

The eigenvalues computed by DRAGON for the cases of uranium oxide (UOX) fuel and mixed-oxide (MOX) fuel are shown in Table 2 and compared with MCNP-3A, MCNP-4A continuous-energy Monte Carlo code with different libraries. On average, the DRAGON eigenvalues have an approximately constant difference comparable to the corresponding MCNP sample mean value. The DRAGON eigenvalues can be compared with the mean values obtained with the Monte Carlo code and expressed by the following relation:

$$K_{\infty,DRAGON} = (\overline{K}_{\infty,MCNP} + Const) \pm \delta \qquad (1)$$

where Const and δ are the constant bias and the standard deviation separately.[7] The corresponding constant biases and standard deviations of DRAGON code with four options were summarized and compared with other transport theory codes[10-12] in Table 3.

Compared with WIMS-AECL results, all DRAGON calculations give eigenvalues with larger bias and larger standard deviation relative to the average eigenvalue predicted by MCNP-3A with ENDF/B-V library for UOX fuel. However, the conclusion is opposite if MCNP-4A eigenvalue were used as the reference. We note that most DRAGON eigenvalues for UOX fuel, including other transport theory codes except WIMS-AECL, are in better agreement with MCNP-4A results than with MCNP-3A results, no matter which kind of libraries were applied.

For UOX fuel, DRAGON calculation of option 1, i.e., self-shielding without LJ normalization based on ENDF/B-VI library, produces the most accurate results among four options. The bias and standard deviation are −2.9 mk and 0.8 mk separately. In this case, the recent MCNP-4A results with ENDF/B-VI library was used as the reference. For MOX fuel, however, we have to use MCNP-3A results with ENDF/B-V library as the reference because it is the only published reference results readily available. In this case, DRAGON calculation of option 1 produces relatively higher bias and standard deviation than those predicted by DRAGON calculation with option 2, i.e., self-shielding with LJ normalization based on ENDF/B-VI library. Its suggests us to use option 1 for UOX fuel calculation, and use option 2 for MOX fuel calculation.

It is important to mention that since we have a nearly constant bias relative to corresponding Monte Carlo calculations, the Doppler coefficients of reactivity are in good agreement with the Monte Carlo calculations.

B. PWR Assembly

Based on the model described in section III, a 17x17 French standard 900 MWe PWR fuel assembly and a BP assembly at beginning of life state were modeled in DRAGON. The DRAGON eigenvalues with four different options were compared with the reference values[13] calculated by Westinghouse commercial PWR nuclear design code PHOENIX-P. We note that DRAGON calculations generally produce more accurate eigenvalues with ENDF/B-VI library than with ENDF/B-V library. DRAGON calculations of option 1 are about

1 mk deviation for PWR fuel assembly and 10 mk for BP assembly. On the contrary, DRAGON calculations of option 2 are about 7.6 mk deviation for PWR fuel assembly and 3 mk for BP assembly. It suggests us to use option 1 for PWR fuel assembly calculation, and use option 2 for PWR BP assembly calculation.

In conclusion, our results showed that the previous approximation made for the PWR assembly modeling was entirely adequate. The JMPT/SYBILT method in DRAGON code, together with the ENDF/B-VI nuclear data library, can predict K–infinity of PWR assemblies with good accuracy. Since the reference feed material used for the DUPIC fuel cycle is only a spent PWR fuel assembly, with 3.2 w/o initial enrichment and 32500 MWD/T discharge burnup, we will use option 1, i.e., self-shielding without LJ option in DRAGON based on ENDF/B-VI library, for our DUPIC fuel cycle study.

V. GENERATION OF NUCLIDE FIELDS IN SPENT PWR FUEL

Assumptions are made during generation of nuclide fields in spent PWR fuel. First, we know that nuclide fields are strongly depend on discharge burnup for a given PWR assembly type, where burnup can be expressed as the integral of assembly power on time domain. Even though the operation history such as soluble boron let down curve, power level, moderator temperature and fuel temperature can affect spectrum and assembly-homogenized macroscopic cross sections, their influence on the assembly-averaged nuclide fields in spent PWR may be neglected. The nominal discharge burnup of reference spent PWR fuel with 3.2 w/o enrichment was chosen to be 32500 MWD/T, which is typical of the 900 MWe Daya Bay PWR plant[5].

Usually, PWR fuel assemblies are burnt for three cycles before discharge, during which they experience different operating history, especially different SB letdown curve. Accurate model SB letdown curve is required for nuclear design but is not necessarily required for nuclide field generation. Here, the reference PWR assembly is subjected to three successive burnup cycles at nominal conditions with an approximated soluble boron letdown curve, shown in Figure 3, simulating the power history of an average assembly. Then a depletion calculation is carried out over three burnup cycles till the nominal discharged burnup(32500 MWD/T) is reached. During the depletion calculation, only one type of fuel mixture with a constant power density, fuel temperature and coolant density is considered.

Finally, a 10-year cooling period is simulated at cold zero power condition. Because of the relatively short half-life of Pu-241 (14.7 y), the fuel composition of the reference spent PWR fuel changes significantly after 10 years of cooling. The resulting nuclide fields (actinides and fission products) will constitute the reference DUPIC initial fuel composition for CANDU cluster cell and supercell calculations. They were saved as XSM database which can be accessed directly by the DRAGON code for CANDU lattice calculation.

VI. FUEL COMPOSITION HETEROGENEITY IN SPENT PWR FUEL

Because of uneven spatial power distribution in PWR assemblies and full core, unexpected transition cycle and various fuel management strategy, the spent PWR fuel conditions such as initial enrichment and discharged burnup are not always the same as the reference one given above. This will result in variations of spent PWR fuel composition from one assembly to next. Such composition heterogeneity of spent PWR fuels were characterized here by calculating various spent PWR fuel assembly types as shown in Table 5. The U235 and PU239 contents after depletion and 10 years cooling calculated with ENDF/B-V and ENDFB/VI libraries are also summarized and compared in Table 5.

Figures 4 to 8 illustrate the variation of PWR fuel composition on initial enrichment, presence of burnable poison, axial position, soluble boron letdown curve and power history. From these figures the effect of spent PWR assembly conditions on PWR fuel composition are observed:

1) The fuel compositions are mainly functions of initial enrichment and discharge burnup. The higher initial enrichment of PWR fuel, the more fissile materials exist in the spent fuel. Lower discharge burnup also leaves more fissile materials in spent fuel. It was interesting to note that, after buunup of 25,000 MWD/T, the number densities of main actinides always change as a linear function of burnup as shown in Figure 4. This implies that simply mixing fuel powders of spent PWR assemblies with different discharge burnup after the OREOX process can eliminate heterogeneity in some extent, as we discussed in a recent paper.[5]

2) For the same initial enrichment and discharge burnup conditions, the fuel compositions (such as number densities of U235 and Pu239 illustrated in Figure 5) are different for fuel assembly and BP assembly. Therefore, the use of BP in modern PWR fuel management strategy will produce extra fuel composition heterogeneity in the spent PWR fuel.

3) The fuel compositions (such as number densities of U235 and Pu239 illustrated in Figure 6) vary largely in different axial position of an assembly at the same operation days. The main reason is that the accumulated burnup distribution varies with axial position because of uneven axial power shape, axial coolant density and axial fuel temperature distributions. The effect of various burnup histories in axial position on fuel composition is relatively small, as shown in Figure 7.

4) The fuel compositions are slightly sensitive to soluble boron letdown curve via neutron spectrum effect as shown in Figure 8.

VII. 2D CANDU CLUSTER CELL DEPLETION AND 3D CANDU SUPERCELL CALCULATION

After PWR assembly depletion and 10 years cooling calculation, DRAGON produces initial fuel composition database for DUPIC fuel which can be accessed directly by the DRAGON code for CANDU lattice analysis. The 2D CANDU cluster cell depletion calculation was done by EXCEL model (collision probability method for both self-shielding and 2D Cluster geometry transport calculation) in DRAGON with ENDF/B-VI library to generate burnup-dependent few group base cross sections for DUPIC fuel. Compared to the standard 37-element CANDU fuel bundle, the DUPIC fuel bundle adopts an advanced CANDU bundle geometry,[14] which has 8 large and 35 small fuel rods, developed as a carrier for the future CANDU fuel to enhance fuel performance and thermal margins. Also 5.27 at% of natural dysprosium is mixed with the center rod to reduce the coolant void reactivity of DUPIC fuel bundle.

The lattice K-infinities of various DUPIC fuels are illustrated in Figure 9 and compared with that of natural uranium fuel. It is clear that all DUPIC fuels have much higher reactivity than natural uranium. The lower the discharged burnup in spent PWR fuel, the higher the lattice K-infinity in corresponding DUPIC fuel.

Following the 2D CANDU cluster cell calculations, a 3-D CANDU supercell calculation is required to model the reactivity devices present in a CANDU reactor such as adjuster rods and zone control units(ZCUs). The incremental cross sections, defined as the difference in macroscopic cross sections of a lattice with and without the reactivity device, were carried out by EXCEL model also in DRAGON with ENDF/B-VI library. For calculational simplicity, we assume here the incremental cross sections were invariant upon burnup and calculated only for equilibrium core conditions.

VIII. CONCLUSION

By using the DRAGON procedures described above, the DUPIC fuel properties such as the base cross sections of DUPIC fuel and incremental cross sections for adjuster rods and ZCUs for 3D core analysis were

generated by DRAGON code and 89 group ENDF/B-VI library consistently. The drawback of using potentially inconsistent computational codes and corresponding libraries of previous studies is overcome. Such cross sections can be used as standard input in the DONJON[15] code, which uses the TRIVAC module[16] to perform 3D CANDU full core diffusion calculations in two energy groups. The previous full core results which using cross sections generated from ENDF/B-V library indicate that the reference DUPIC fuel can be loaded in the current CANDU-6 without significant modification of the reactor system or performance requirement.[5] However, in order to make the DUPIC fuel cycle practical, the fuel composition heterogeneity in spent PWR fuel observed in this paper has to be addressed.

ACKNOWLEDGMENTS

The authors are grateful to G. Marleau and R. Roy for their useful discussions and advice in modeling PWR assembly and Mosteller benchmark problem with DRAGON.

REFERENCES

1. M. S. Yang et al., "Conceptual Study on the DUPIC Fuel Manufacturing Technology", *Proc. Int. Conf. And Technology Exhibition on Future Nuclear System: Emerging Fuel Cycles and Waste Disposal Options, GLOBAL '93*, Seattle, Washington (1993).
2. H. B. Choi, B. W. Rhee, et al., "Fuel Composition Heterogeneity analysis", *Proc. Int. Conf. on the physics of Reactors, PHYSOR96*, Sept. 16-20, 1996, p. I 114, Mito, Ibaraki, Japan (1996).
3. G. Marleau, A. Hebert, R. Roy, *A User's Guide for DRAGON*, Report IGE-174 Rev. 3, Ecole Polytechnique de Montreal, Canada (1997).
4. R. Roy, G. Marleau et al, "Modelling of CANDU Reactivity Control Devices with the Lattice Code DRAGON", *Ann. Nucl. Energy*, **21**, 115, 1994.
5. W. Shen, D. Rozon, "Study of DUPIC Fuel Cycle in CANDU-6 Reactors Using DRAGON/DONJON", *Int. Conf. on the physics of Nuclear Science and Technology*, New York, USA, Oct. 5-8,1998.
6. G. Marleau, *A First Validation of the Code DRAGON for the Winfrith Library Using the Chark River Experimental Database*, IGE-182 Rev. 1, Ecole Poly-technique de Montreal, Canada (1996).
7. R. D. Mosteller, L. D. Eisenhart, et al, "Benchmark Calculations for the Doppler Coefficient of Reactivity", *Nucl. Sci. Eng.*, **107**, 265, 1991.
8. R. D. Mosteller, J. T. Holly, et al, "Benchmark Calculations for the Doppler Coefficient of Reactivity in Mixed-Oxide Fuel", *Proc. Of Int. Tpl. Mtg. On Advances in Mathematics, Computations and Reactor Physics*, Vol 2, Aril 28 - May 2, 1991, Pittsburgh, USA (1991).
9. F. Rahnema, H. M. Gheorghiu, "ENDF/B-VI Benchmark Calculation for the Doppler Coefficient of Reactivity", *Ann. Nucl. Energy*, **23**, 1011, 1996.
10. F. C. Wong, "WIMS-AECL Calculations for the Doppler Coefficient of Reactivity", *Can. Nucl. Soc. 13th Ann. Conf.*, Vol 1, June 7-10, 1992, Saint John, New Brunswick, Canada (1992).
11. I. Soares, W. F. Miller and R. T. Perry, "Analysis of ONEDANT Code Package for the Calculation of Doppler Coefficient of Reactivity", *Nucl. Sci. Eng.*, **114**, 160, 1993.
12. M. Edenius, "CASMO Doppler Coefficients Versus MCNP-3A Monte Carlo Calculations", *Trans. Am. Nucl. Soc.*, **70**, 348, 1994.
13. S. Xie, Private communication, July 1997.
14. I. J. Hastings, A. D. Lane, P. G. Boczar, "CANFLEX – An Advanced Fuel Bundle for CANDU", *Proc. Int. Conf. on Improvements in Availability of Nuclear Power Plants*, April 8-11, 1989, Madrid, Spain (1989). Also AECL-9029 (1989).
15. E. Varin, A. Hebert, R. Roy, J. Koclas, *A User's Guide for DONJON*, Report IGE-208, Ecole Poly-technique de Montreal, Canada (1996).

16. A. Herbert, "TRIVAC: A Modular Diffusion Code for Fuel Management and Design Application", *Nucl. J. of Canada*, **1**, 4 (1987).

Table 2: Comparison of DRAGON Eigenvalue for PWR Pin Cell Geometry with Uranium Oxide(UOX) and Mixed-Oxide(MOX) Fuels

Enr. (wt%)	Fuel Temp (K)	MCNP-3A ENDF/B-V	MCNP-4A ENDF/B-V	MCNP-4A ENDF/B-VI	DRAGON No LJ ENDF/B-VI	DRAGON LJ ENDF/B-VI	DRAGON No LJ ENDF/B-V	DRAGON LJ ENDF/B-V
0.711	600	0.6638±0.0006	0.6661±0.0003	**0.6668±0.0003**	**0.6645**	0.6696	0.6614	0.6667
	900	0.6567±0.0008	0.6589±0.0003	**0.6593±0.0003**	**0.6567**	0.6520	0.6533	0.6587
1.6	600	0.9581±0.0006	0.9612±0.0004	**0.9628±0.0004**	**0.9602**	0.9677	0.9542	0.9618
	900	0.9484±0.0006	0.9519±0.0004	**0.9545±0.0004**	**0.9502**	0.9579	0.9437	0.9516
2.4	600	1.0961±0.0007	1.0996±0.0004	**1.1023±0.0004**	**1.0995**	1.1079	1.0913	1.0999
	900	1.0864±0.0007	1.0897±0.0004	**1.0920±0.0004**	**1.0889**	1.0976	1.0801	1.0889
3.1	600	1.1747±0.0007	1.1782±0.0004	**1.1809±0.0004**	**1.1789**	1.1877	1.1689	1.1779
	900	1.1641±0.0006	1.1667±0.0004	**1.1711±0.0004**	**1.1680**	1.1771	1.1574	1.1666
3.9	600	1.2379±0.0006	1.2411±0.0005	**1.2451±0.0005**	**1.2433**	1.2524	1.2314	1.2407
	900	1.2271±0.0006	1.2295±0.0005	**1.2362±0.0005**	**1.2323**	1.2417	1.2197	1.2292
Pu Con. (a/o)	Fuel Temp (K)	MCNP-3A ENDF/B-V			DRAGON No LJ ENDF/B-VI	DRAGON LJ ENDF/B-VI	DRAGON No LJ ENDF/B-V	DRAGON LJ ENDF/B-V
1.0	600	0.9445±0.0007			0.9382	**0.9454**	0.9364	0.9439
	900	0.9347±0.0007			0.9281	**0.9355**	0.9264	0.9341
2.0	600	1.0182±0.0007			1.0092	**1.0167**	1.0072	1.0149
	900	1.0077±0.0007			0.9989	**1.0066**	0.9967	1.0046

Table 3: Deviation of Calculated Eigenvalues from Monte Carlo Results

Reference Results		MCNP-3A, ENDF/B-V		MCNP-4A, ENDF/B-V		MCNP-4A, ENDF/B-VI	
Lattice Code	Fuel Type	Constant Bias	Standard Deviation	Constant Bias	Standard Deviation	Constant Bias	Standard Deviation
DRAGON (No LJ, ENDF/B-VI)	UOX	0.0029	0.0017	0.0000	0.0016	**-0.0029**	**0.0008**
	MOX	-0.0077	0.0012				
DRAGON (LJ, ENDF/B-VI)	UOX	0.0098	0.0055	0.0069	0.0052	0.0041	0.0040
	MOX	**-0.0002**	**0.0011**				
DRAGON (No LJ, ENDF/B-V)	UOX	-0.0052	0.0015	-0.0082	0.0017	-0.0011	0.0033
	MOX	-0.0096	0.0014				
DRAGON (LJ, ENDF/B-V)	UOX	0.0029	0.0006	-0.0001	0.0004	-0.0029	0.0020
	MOX	-0.0019	0.0013				
WIMS-AECL (DSN, ENDF/B-V)	UOX	0.0002	0.0005	-0.0028	0.0006	-0.0056	0.0022
	MOX	-0.0045	0.0011				
CELL-2 (ENDF/B-V)	UOX	0.0021	0.0005	-0.0008	0.0003	-0.0037	0.0016
	MOX	0.0034	0.0011				
ONEDANT (ENDF/B-V)	UOX	0.0048	0.0010	0.0018	0.0007	-0.0010	0.0013
CASMO-4 (ENDF/B-V)	UOX	0.0031	0.0007	0.0001	0.0008	-0.0027	0.0024

Table 4: Benchmark of DRAGON Eigenvalues for PWR Assemblies

Enr. (wt%)	BP Rods	Reference	No LJ ENDF/B-VI	LJ ENDF/B-VI	No LJ ENDF/B-V	LJ ENDF/B-V
3.11	0	1.19767	**1.19657**	1.20530	1.18544	1.194342
3.11	16	1.05074	1.04022	**1.04772**	1.03032	1.03797

Table 5: Number Densities ($10^{20}/cm^3$) of U235 and PU239 for Different Spent PWR Fuel Types (After 10 years cooling)

No	Enr. (wt%)	Discharge BU (GWD/T)	Types	ENDF/B-VI Results U235	ENDF/B-VI Results PU239	ENDF/B-V Results U235	ENDF/B-V Results PU239
1	3.2	30	Nominal, No BP	2.310	1.312	2.319	1.335
2	3.2	32.5	Nominal, 16 BP	2.252	1.566	2.266	1.596
3	**3.2**	**32.5**	**Nominal, No BP**	**2.069**	**1.328**	**2.080**	**1.353**
4	3.2	32.5	Top, No BP	2.387	1.285	2.394	1.309
5	3.2	32.5	Center, No BP	1.551	1.375	1.568	1.406
6	3.2	32.5	Bottom, No BP	2.369	1.313	2.378	1.332
7	3.2	35	Nominal, No BP	1.848	1.340	1.861	1.366
8	3.5	35	Nominal, No BP	2.245	1.375	2.255	1.400

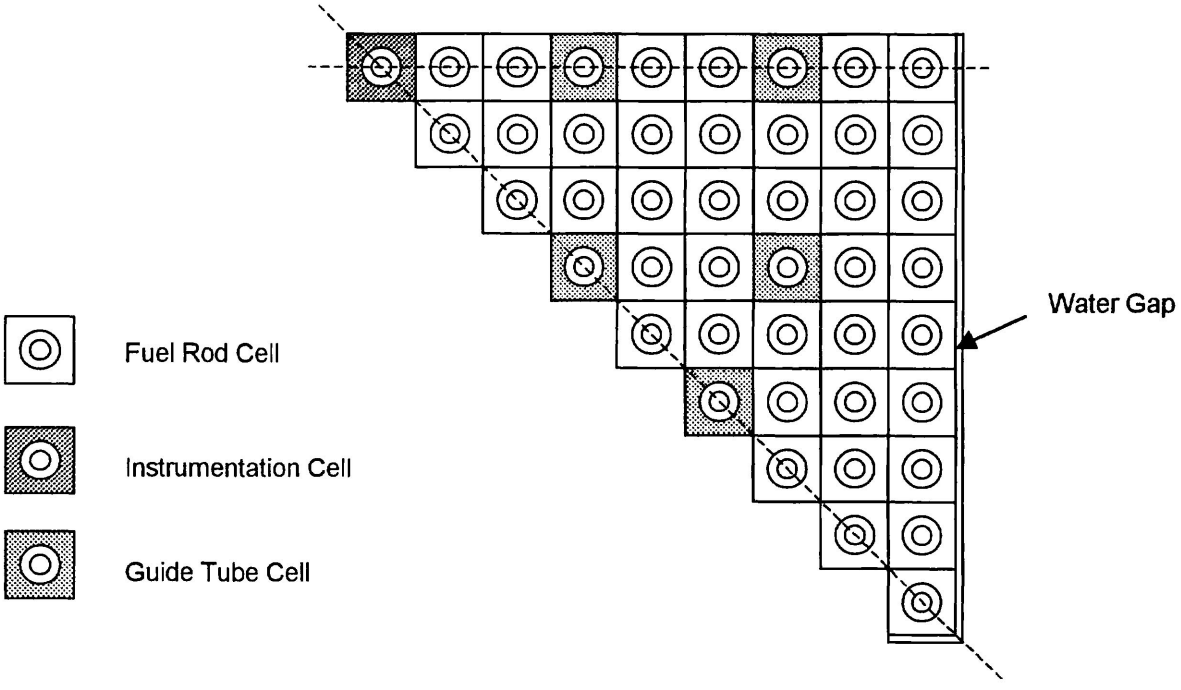

Figure 1: Geometry of One-Eighth PWR Fuel Assembly

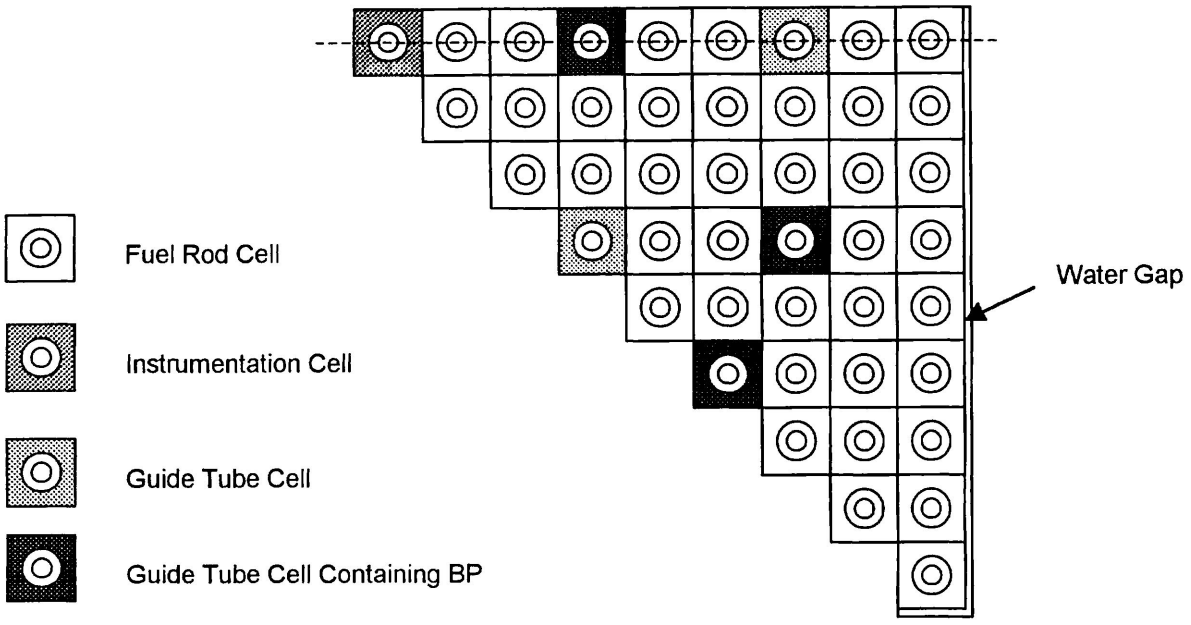

Figure 2: Geometry of One-Eighth PWR BP Assembly

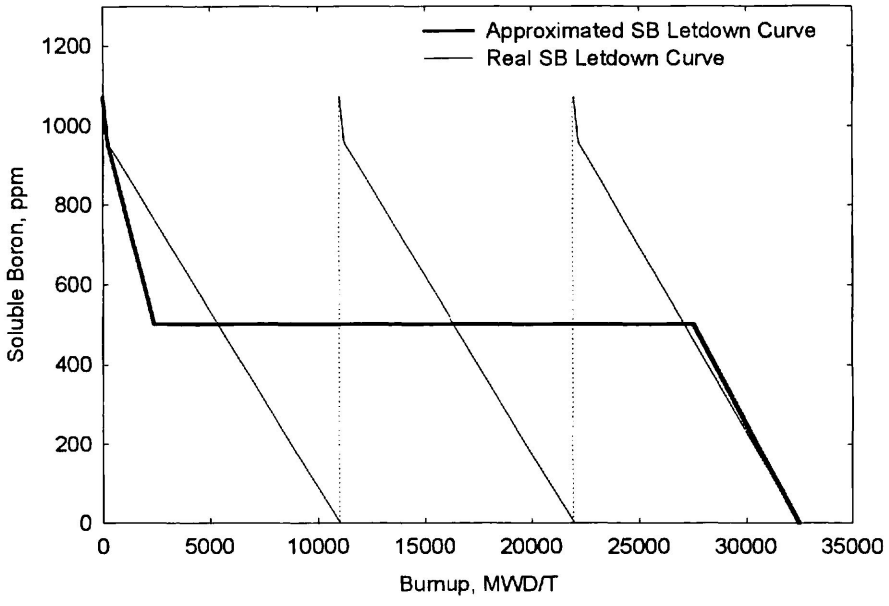

Figure 3: Soluble Boron Letdown Curve in PWR Fuel Assembly (3.2 w/o)

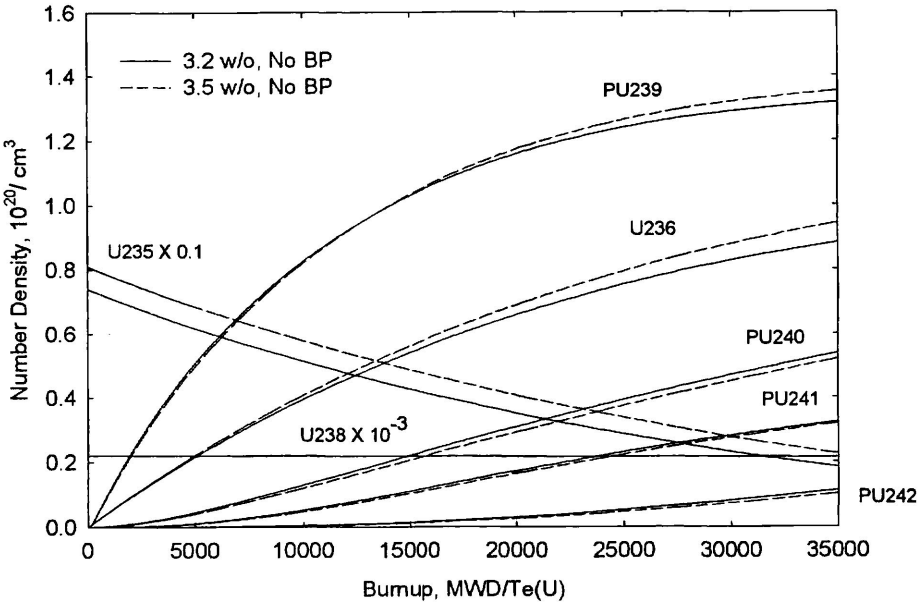

Figure 4: PWR Fuel Composition: Initial Enrichment

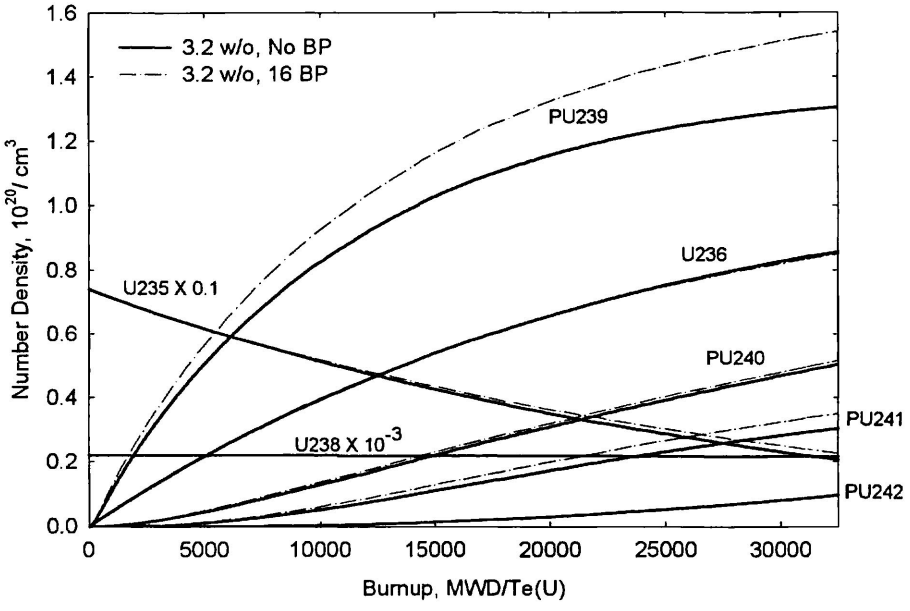

Figure 5: PWR Fuel Composition: Presence of Burable Poison (BP)

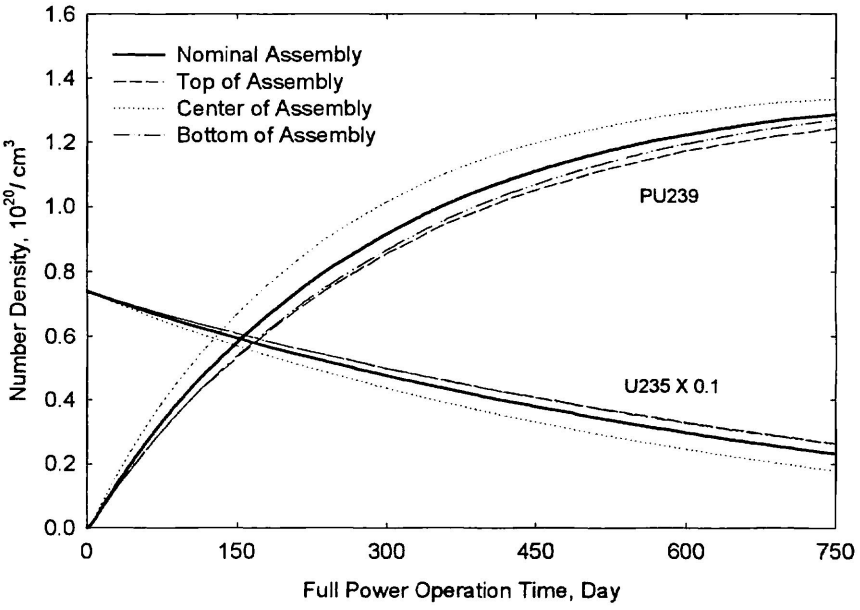

Figure 6: Variation of PWR Fuel Composition versus Operation Time (3.2 w/o, No BP)

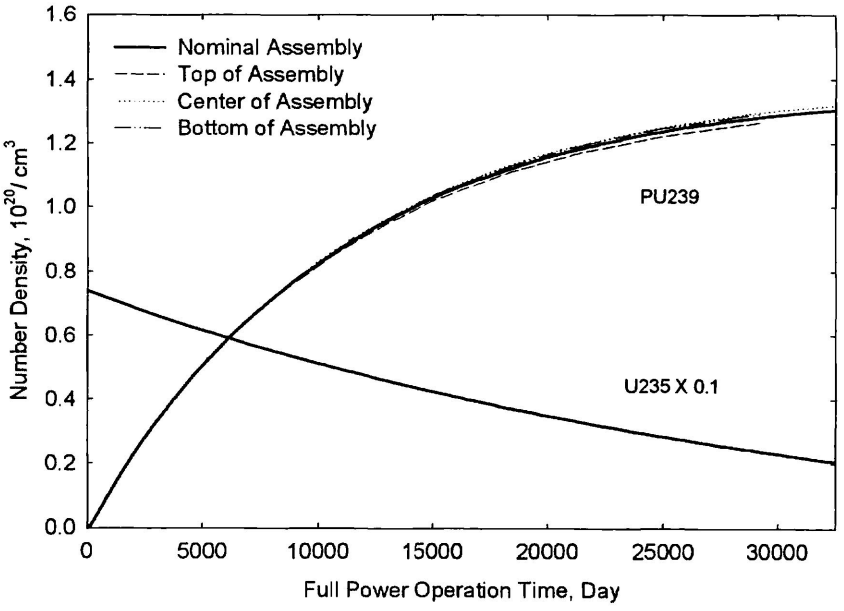

Figure 7: Variation of PWR Fuel Composition versus Burnup (3.2 w/o, No BP)

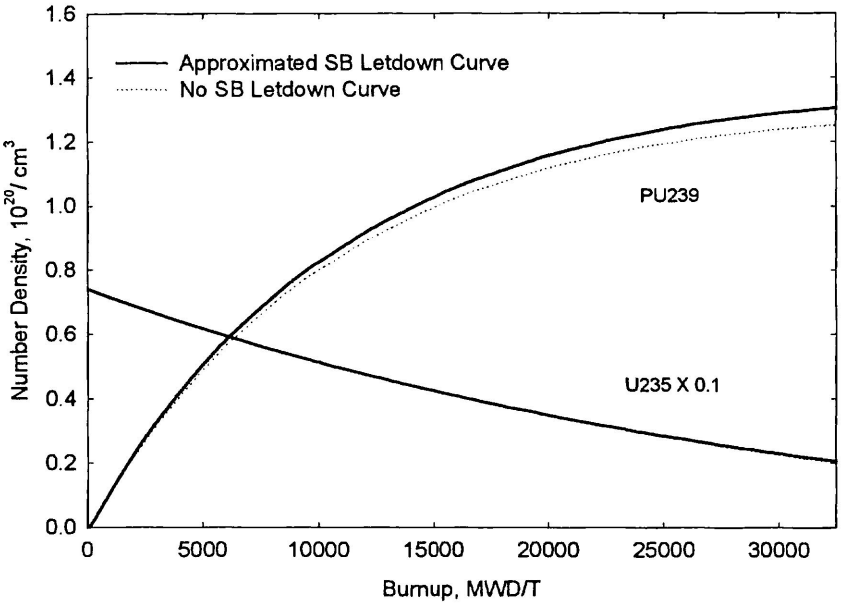

Figure 8: PWR Fuel Composition: Influence of Soluble Boron (3.2 w/o, No BP)

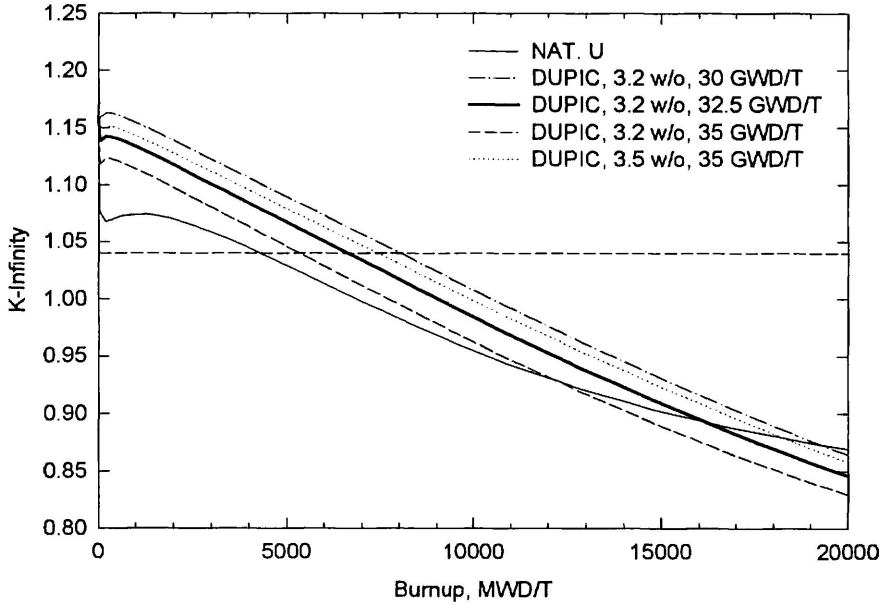

Figure 9: CANDU Lattice K-infinity for Different DUPIC Fuel Types